Combined process automation for large-scale EEG analysis

John L. Sfondouris [a], Tabitha M. Quebedeaux [a], Chris Holdgraf [b], Alberto E. Musto [a,*]

[a] *Neuroscience Center of Excellence, Louisiana State University Health Sciences Center, 2020 Gravier Street, Suite D, New Orleans, LA 70112, USA*
[b] *Graduate School, Helen Wills Neuroscience Institute, University of California, Berkeley, 424 Sproul Hall #5900, Berkeley, CA 94720, USA*

ARTICLE INFO

ABSTRACT

Epileptogenesis is a dynamic process producing increased seizure susceptibility. Electroencephalography (EEG) data provides information critical in understanding the evolution of epileptiform changes throughout epileptic foci. We designed an algorithm to facilitate efficient large-scale EEG analysis via linked automation of multiple data processing steps. Using EEG recordings obtained from electrical stimulation studies, the following steps of EEG analysis were automated: (1) alignment and isolation of pre- and post-stimulation intervals, (2) generation of user-defined band frequency waveforms, (3) spike-sorting, (4) quantification of spike and burst data and (5) power spectral density analysis. This algorithm allows for quicker, more efficient EEG analysis.

© 2011 Elsevier Ltd. All rights reserved.

1. Introduction

Animal models of epilepsy provide a means of studying the progressive neuropathological changes associated with epileptogenesis and gauging the effectiveness of potential treatments. The electrical discharges from the brain are useful for diagnosing epilepsy and monitoring anti-epileptic treatments [1,2].

Electrical stimulation of the rodent hippocampus evokes a burst of electrical activity known as an afterdischarge (AD), which contains distinct phases of unique electroencephalographic (EEG) morphology [3,4]. The electrical activity produced by stimulation of rodents that have previously undergone epileptogenesis using the rapid kindling model is characterized by robust changes in the morphology of each phase of the AD [5]. Analyzing these patterns through both qualitative and quantitative measures is essential to further characterizing differences in the response to stimulation between normal and epileptic brains, as well as in evaluating the effectiveness of potential anticonvulsive and antiepileptogenic treatments.

Powerful tools and software for EEG analysis make highly complex and detailed data processing possible; however, manually implementing these tools to process and analyze individual EEGs for a large data set is time-consuming and repetitive. Waiting for individual processes to run between user commands is cumbersome, and the time loss due to human response, menu navigation and command execution accumulates rapidly with repetitive user input. This can make large-scale data analysis highly inefficient, increase the possibility for human error and lead to data backlog and research delays. Since the majority of time lost to inefficiency is accrued by the user, limiting the need for user input through the use of automated processes should greatly improve data processing efficiency.

In the current study, the goal is to develop a tool to be used for EEG analysis in experimental models of epilepsy with the potential for clinical translation. Thus we describe an algorithm designed to streamline EEG data analysis by providing linked automation of several aspects of data processing. EEG recordings were collected from a series of 14 electrical stimulations to the right dentate gyrus of rats. Recordings were processed using NeuroExplorer, and automated processes were created using NexScript software (Nex Technology, Littleton, MA, USA). The algorithm enables more efficient and comprehensive EEG utilization to be accomplished virtually unsupervised directly from the raw EEG.

2. Materials and methods

Studies were performed on 6 adult male Wistar rats (8 weeks old; Charles River Laboratories, Wilmington, MA, USA) in accordance with the National Institutes of Health Guide for the Care and Use of Laboratory Animals. Protocols were approved by the Louisiana State University Health Sciences Center Institutional Animal Care and Use Committee. Animals were housed individually in a temperature-controlled vivarium under a 12-hour light/dark cycle and were provided access to food and water *ad libitum*.

Animals were allowed to acclimate to their surroundings upon arrival to the animal facility prior to undergoing surgery.

2.1. Surgery

Animals were anesthetized with a mixture of ketamine hydrochloride and xylazine (50–80 mg/kg and 5–8 mg/kg; i.p.) and secured in a stereotaxic frame. Bipolar electrodes (Plastics One, Roanoke, VA) were implanted in the right dentate gyrus (AP: −3.6 mm, L: 2.0 mm, DV: 4.0 mm ventral to the dura) [6]. Electrodes were grounded to a single screw implanted in the occipital bone. All implanted hardware was fixed in position to the skull with acrylic glue. Following surgery, animals were returned to individual cages and allowed 7 days to recover prior to stimulations.

2.2. Stimulation and EEG recording

Rats were transferred to Plexiglas cages and allowed to freely roam during subsequent stimulations and EEG recordings. Each rat's bipolar electrode was connected to the data acquisition system by a series of cables linked through a commutator. The stimulation protocol consisted of a single series of 14 electrical stimulations (10-s train of 50 Hz biphasic 1-ms pulses) [7] delivered at 30-min intervals via the bipolar electrode to the right dentate gyrus. The stimulation intensity was graduated with the first six stimulations at 50 µA, the next six at 100 µA and the final two at 200 µA. This stimulation protocol was implemented to detect differences in AD responses associated with limbic seizures. The gradation is intended to illicit different threshold-specific responses that are of use when comparing the stimulation data of normal rats and epileptic rats with and without anti-epileptogenic and anticonvulsive treatments. Synchronous five-minute video (JVC Everio, Wayne, NJ, USA) and EEG recordings were collected for each stimulation. Recordings were composed of a short pre-stimulation segment continuous with the immediate post-stimulation period such that each recording included at least 50 s of pre-stimulation EEG for baseline comparison and at least 160 s of post-stimulation EEG. Stimulations were delivered sequentially to 6 animals over approximately 90 s, and EEG recordings were collected using Enhanced Graphics Acquisition for Analysis (Version 3.63, RS Electronics, Santa Barbara, CA). The signal was amplified 1000 times, band-pass filtered 0.5–40 Hz (3 dB/octave; Med Associates, Georgia, VT, USA) and digitized at a sampling rate of 200 Hz. Two skilled observers continuously monitored rat behavior, and post-stimulation behavioral responses were graded using a modified Racine Scale [8] (data not included). Upon completion of the stimulation series, animals were deeply anesthetized [ketamine hydrochloride (50–80 mg/kg) and xylazine (5–8 mg/kg); i.p.] and sacrificed.

2.3. Data analysis

EEG data was visualized and subsequently analyzed offline using NeuroExplorer (Nex Technology, Littleton, MA). The selected AD segment or burst, which was defined to include clusters of repetitive epileptiform potentials (spikes, poly-spikes, spike-waves and sharp waves), was manually selected, and the initiation and conclusion of the AD were entered as interval data into the NeuroExplorer file [9].

2.4. Programming

Code for the algorithm and automated processes was written in NexScript (Nex Technology, Littleton, MA) and functions through the use of NeuroExplorer to access and modulate files containing EEG data. The code for the master script may be found in the Appendix.

3. Results and discussion

3.1. Algorithm design

Numerous studies have focused on automated EEG analysis to determine the best and most efficient method to identify specific events such as spikes and seizures [10,11]. We designed an algorithm that combines several tools and techniques to automate data processing and analysis for an entire data set. The goal was to create a standardized, adaptable system for use in experimental epilepsy models that optimizes EEG utilization and minimizes the burden on the electroencephalographer. The algorithm is designed to be modular, and each step of data analysis (Fig. 1) is performed by a separate automated routine or script. A single master script (Appendix) controls all the individual scripts and provides the interface through which all user input to the algorithm is entered. Here the user specifies which modules to run, where output files are saved and what parameters are used for the active modules. With the exception of the 'Spike & Burst Analysis' and 'power spectral density (PSD) Analysis' phases, which utilize manually selected AD burst intervals, modules can be executed without prior modification to the raw data.

3.1.1. EEG alignment to the stimulus and extraction of pre- and post-stimulation intervals

The sequential method by which our setup delivers stimulations to the animals aids in behavior analysis by temporally separating individual behavioral responses, thereby facilitating real-time observation of multiple animals simultaneously. However, EEG alignment relative to the point of stimulation facilitates the comparison of AD progression between animals and among stimulations for the same animal. The 'EEG Event Alignment' phase of the algorithm aligns the EEGs relative to the point of stimulation by locating the initial amplitude spike of the stimulation event for a single user-specified channel and using its position in the sequence to synchronize the stimulation times for all channels (Fig. 2A). Because the algorithm is modular, this
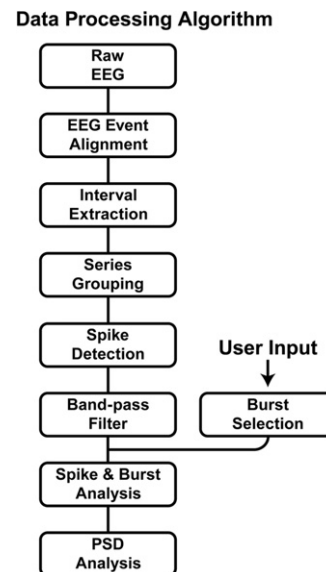

Fig. 1. Flow diagram of the data processing algorithm. Each processing step is coded in an independent script controlled through a master script that accepts all user inputs. The master script may be utilized to run individual or multiple scripts. Additional process scripts controlled by the master script (not shown) offer the option of automatically exporting rasters as well as batch removal of user-specified variables from multiple files.
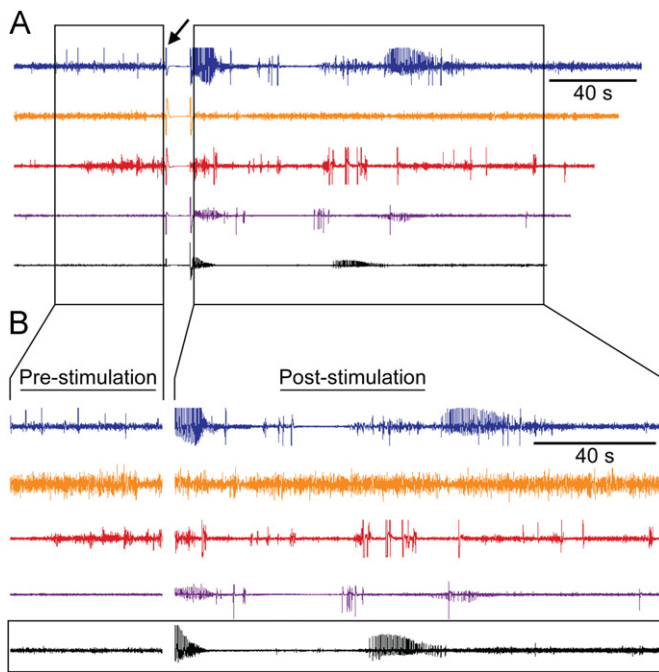
Fig. 2. EEG alignment to the stimulus and interval extraction output: (A) the 5 EEG recordings represent responses of 5 animals to right dentate gyrus stimulation that have been temporally aligned relative to the start of their respective stimulations (arrow). The black boxes encompass the standardized pre- and post-stimulation EEG segments to be isolated and (B) the isolated segments are shown with a box marking the EEG that will be further analyzed in subsequent figures. Time scale is shown for each EEG; amplitude scale varies by EEG based on the maximum and minimum amplitude values for each.
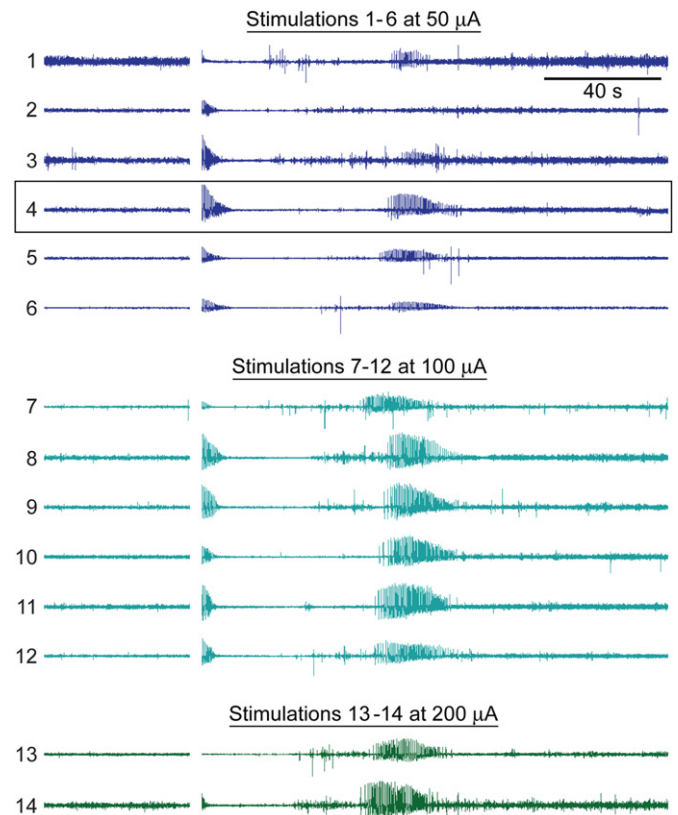

Fig. 3. Series grouping output. The full series of 14 pre- and post-stimulation EEGs are shown in ascending order for a single animal with stimulations 1–6 at 50 μA, 7–12 at 100 μA and 13–14 at 200 μA. The fourth stimulation, marked with a box, is the same as that marked in Fig. 2B, here shown in the context of stimulations to a common animal. Time scale is shown for each EEG; amplitude scale varies by EEG based on the maximum and minimum amplitude values for each.

phase can be run in isolation within minutes of the completion of each recording, allowing one to actively assess the progression of ADs over the series of the stimulations, appreciate trends and contextualize corresponding behavioral responses. The 'EEG Event Alignment' phase may also be modified to align other events of interest, such as seizures, for comparison.

Once EEGs have been aligned, the 'Interval Extraction' phase of the algorithm isolates the 50-s segment occurring immediately prior to the stimulation and the corresponding 160-s post-stimulation segment that starts immediately following the gross return of the mean EEG signal to baseline (Fig. 2B). The interval lengths and positions relative to the stimulation can be adjusted to fit the user's needs. This phase of the algorithm defines and standardizes the pre- and post-stimulation intervals relative to the stimulation and vastly reduces the time requirement from that of manual EEG interval selection. The consistency and reproducibility of pre- and post-stimulation interval selection across all recordings facilitates and enhances both qualitative and quantitative analysis of EEGs.

3.1.2. Organization of EEG data for offline visual analysis

After isolating standardized intervals, visually analyzing a complete series of EEGs remains a daunting task. In the past, methods included alternating between several overlapping windows or poring through large stacks of EEG strips, but the efficiency and ability to follow strip-to-strip trends was somewhat limited or simply time-intensive [12,13]. In our experiment, we delivered a series of 14 stimulations per rat, each generating an individual EEG stored in one of 14 files corresponding to the respective stimulation. To facilitate the analysis of this data, the 'Series Grouping' phase of the algorithm rearranges the EEG data

to create a single file for each animal that contains the EEG recordings from all 14 stimulations in the series (Fig. 3). Upon completion of this phase, the entire sequence of standardized, temporally aligned post-stimulation EEGs can be viewed together on a single monitor. This viewing window allows a more thorough visual analysis without being limited to a specific time scale, as is necessary when EEGs are printed or viewed in separate windows. The analyst can then simultaneously process multiple EEGs within a single viewing window and focus solely on identifying the subtle similarities and differences among them.

3.1.3. Automated creation of frequency bands for analysis

Further analysis of post-stimulation EEG composition, especially AD bursts (see Section 2.3) and their respective oscillatory components, requires application of a band-pass filter to the EEG that isolates user-selected frequency bands. As shown in Fig. 4, the 'Band-pass Filter' phase of the algorithm is useful in analyzing AD waveforms corresponding to delta (0.5–3.5 Hz), theta (4–8 Hz), beta (13–20 Hz) or gamma (21–80 Hz). The new waveforms are stored within the same file to facilitate selection and viewing for analysis. We acknowledge that no consensus exists as to the limits that define the common frequency bands, so we designed this phase to allow the user to modify the frequency band limits as desired. The algorithm is also equipped to isolate additional frequency bands such as ripples and high frequency oscillations. Upon isolation, quantification of ripples and high frequency oscillations is then possible through the 'Spike and Burst Analysis' phase of the algorithm described in Section 3.1.5.
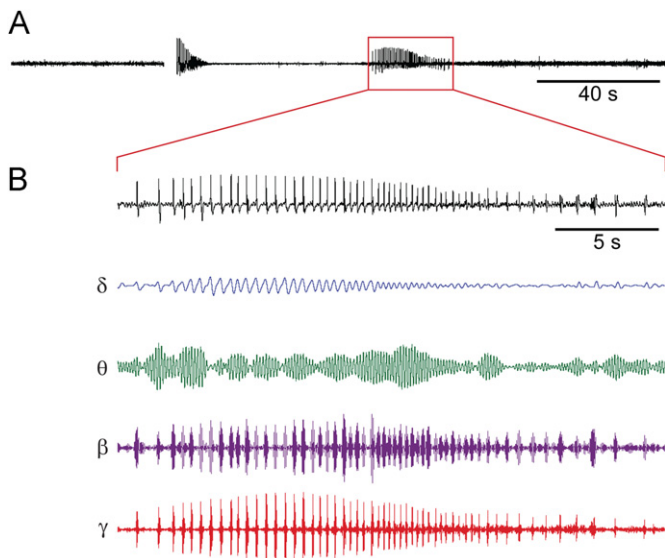
Fig. 4. Band-pass filter output: (A) the EEG marked in Figs. 2B and 3 is shown here. The box contains the selected AD interval for which the isolated band frequency waveforms are shown in (B): delta (δ; 0.5–3.5 Hz), theta (θ; 4–8 Hz), beta (β; 13–20 Hz) and gamma (γ; 21–80 Hz). The spikes in the raw EEG can be seen to correspond to the peaks of δ, β and γ, while θ oscillations, though prominent, do not correspond to peaks. Time scale is shown for each EEG; amplitude scale varies by EEG based on the maximum and minimum amplitude values for each.

3.1.4. Automated spike detection

The 'Spike Detection' phase of the algorithm detects points in the EEG that represent epileptiform potentials. It first identifies possible spikes based on a threshold calculated from the mean and the product of the standard deviation (SD) and a user-defined threshold coefficient [3,10]. The threshold coefficient was set to 2.5 for the current study, yielding a threshold of 2.5 SDs from the baseline amplitude. Each supra-threshold value is then compared to nearby points ensuring that a single spike marks each voltage peak (Fig. 5). This process uses the power (root mean square) of the signal on a sliding window for spike detection. The algorithm also provides the option to perform 'Spike Detection' on any isolated frequency bands created during the 'Band-pass Filter' phase, which can be utilized to study events such as ripples and high frequency oscillations.

3.1.5. Optimization of spike and burst analysis

AD bursts provide further insight into neuronal responses to stimulation. NeuroExplorer has a built-in template that uses multiple parameters applied to the set of marked amplitude spikes to create intervals that approximate AD bursts. Additionally, the template generates numerous quantitative statistics including spike rate (Fig. 6), burst rate, burst duration and spikes/burst. We sought to analyze AD bursts exhibiting clusters of repetitive epileptiform spiking [9]. We were unable to use the template to create a filter with sufficient sensitivity for identifying AD bursts that could still reliably exclude false positives secondary to the combination of non-repetitive spiking and noise-related spikes in our data. However, we were able to achieve adequate burst identification through meticulous manual adjustment of template-derived intervals. Unfortunately, manual adjustment rendered the previously template-derived numerical data obsolete and posed a time requirement similar to that of manually selecting the burst intervals. To obtain the accurate burst intervals needed to generate reliable quantitative data, the
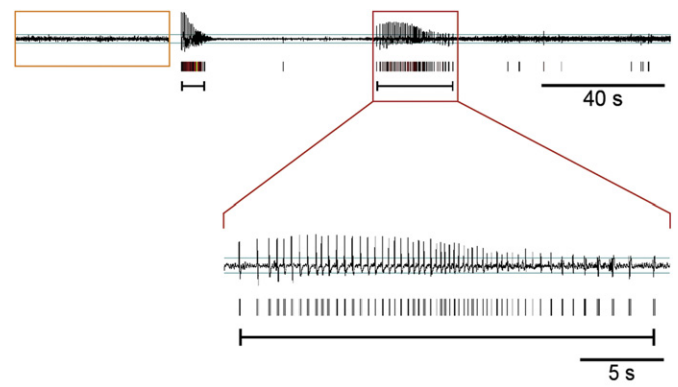

Fig. 5. Spike and burst analysis output. The EEG shown in Fig. 4A is shown with corresponding spikes marked by vertical bars and AD burst intervals marked below spikes. The expanded segment contains the AD interval (square box). The thin pairs of lines represent the spike threshold, which was set at 2.5 standard deviations relative to the mean baseline, and the rectangular box marks the pre-stimulation segment, which exhibits no spike activity. Time scale is shown for each EEG; amplitude scale varies by EEG based on the maximum and minimum amplitude values for each.
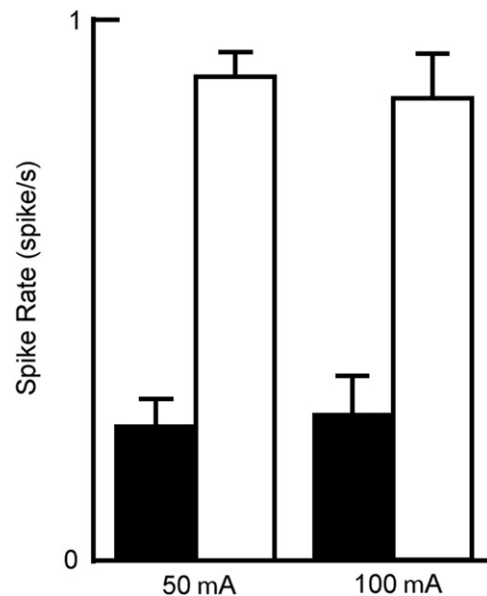

Fig. 6. Spike rate. The bar graph shows the overall pre-stimulation (black) and post-stimulation (white) spike rates for 50 and 100 μA stimulations ($n=35$ and 36 EEGs, respectively). Error bars represent one standard error.

AD burst intervals first need to be selected manually (see Section 2.3, Fig. 1) and then the 'Spike and Burst Analysis' phase of the algorithm uses the built-in template to generate data that corresponds to the manually selected intervals (Fig. 5). The algorithm may easily be modified to utilize automated burst detection and, in such a case, could be run unsupervised and uninterrupted. We have utilized the algorithm in this way for other experiments to quantify ripples or bursts of high frequency oscillations in recordings collected from 16-channel silicon probes (NeuroNexus, Ann Arbor, MI, USA) by a different recording system. As an example, the channels for spike extraction were band-pass filtered between the frequencies of 200 and 300 Hz using a standard Butterworth Filter. The high-frequency data then underwent a spike-detection process. The average signal value was calculated for each channel, and a threshold for spike detection was set at three standard deviations from this mean. A timestamp was placed at every point where the filtered EEG

data crossed this threshold, resulting in multiple trains of spikes that marked high-frequency activity. For burst analysis, groups of spikes that had inter-spike-intervals within ten milliseconds of each other were considered a burst of HFO. A minimum of three spikes was necessary for a train of spikes to be considered a burst. The number of bursts, average length of burst and average spikes per burst that occurred in each channel were then quantified and analyzed (data not included).

3.1.6. Automated power spectral density analysis

Power spectral density (PSD) is another useful tool for characterizing post-stimulation EEGs and has been used extensively in sleep/wake state scoring and seizure detection [12,14]. The relative contributions of the different frequency bands can be determined for an individually specified sequence in NeuroExplorer using a PSD template, which generates graphical and numerical data that can be output in Excel spreadsheets (Microsoft, Redmond, WA, USA). The 'PSD Analysis' phase of the algorithm uses the PSD template to automatically generate PSD data for user-defined EEG segments. Figs. 7 and 8 show how this data can be used to compare a pre-stimulation EEG to an AD burst segment. PSD data may be used similarly to analyze trends among post-stimulation EEG segments, AD bursts or to characterize

Fig. 7. Power spectral density analysis output. The continuous plot shows the percentage of the total power spectral density (PSD) from 0 to 40 Hz for the pre-stimulation segment (orange) and the AD burst interval (red) corresponding to the rectangular and square boxes in Fig. 5, respectively.

Fig. 8. Frequency analysis. The bar graph compares mean PSD values for several of the oscillatory components shown in Fig. 4 with burst interval oscillation values (red) normalized to pre-stimulation values (orange). Note the relative decrease in delta oscillations and increase in beta and gamma oscillations in the AD burst, which is consistent with their appearance in Fig. 4.

different phases of the AD within a single strip. Additionally, the numerical data output to Excel is automatically organized into a logical, easy-to-use format as it is generated. Overall, the algorithm vastly reduces the time requirement for PSD analysis, making it feasible for use in large-scale analysis.

4. Conclusions

The algorithm we developed facilitates data analysis by automating the following steps in EEG data manipulation: (1) alignment and isolation of standardized segments of pre- and post-stimulation EEGs, (2) generation of isolated band-frequency waveforms, (3) spike detection, (4) generation of quantitative data including spike rate, AD burst rate, AD duration and spikes per AD burst and (5) generation of quantitative PSD data from user-defined segments of the EEG recording that can include AD bursts. In addition to increasing the efficiency of each individual phase of data analysis, minimizing the number of interruptions from user-required steps and the extent of user involvement in data processing allows the algorithm to be run virtually unsupervised. Overall, this algorithm enables rapid, large-scale EEG analysis through a customizable framework that facilitates reproducibility and adaptability to new studies.
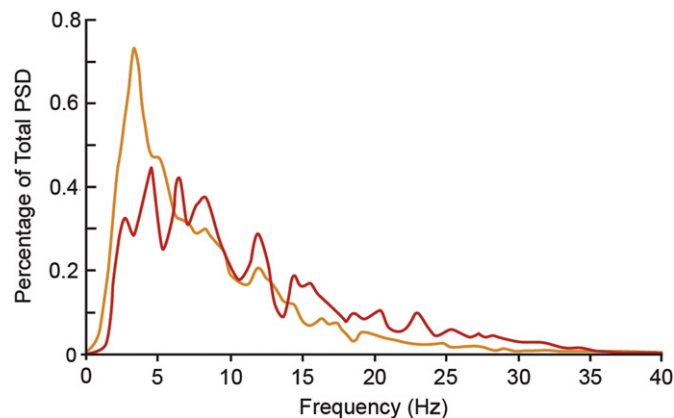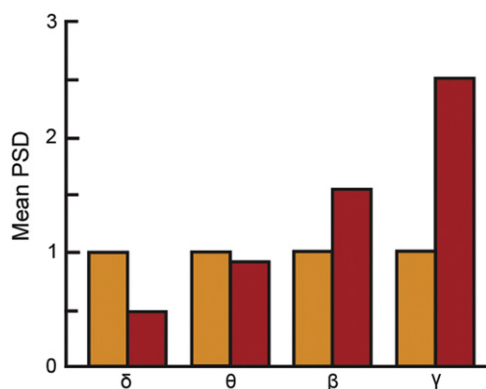
Conflict of interests

None declared.

Appendix A. User-input section of master script

The initial section of the Master Script is presented. It contains the part of the Master Script with which the user will work and in which all the user-specified variables are defined. Non-coding text and characters appear in green and are preceded by '%'. Variables to be defined for use in the code appear in black. The corresponding user definitions appear in red if they represent a number and in blue within quotation marks if they represent a text string.

Appendix B. Supplementary material

Supplementary data associated with this article can be found in the online version at doi:10.1016/j.compbiomed.2011.10.017.

References

[1] P.S. Buckmaster, Laboratory animal models of temporal lobe epilepsy, Comp. Med. 54 (2004) 473–485.
[2] H.S. White, Animal models of epileptogenesis, Neurology 59 (2002) S7–S14.
[3] A.E. Musto, M.S. Samii, J.F. Hayes, Different phases of afterdischarge during rapid kindling procedure in mice, Epilepsy Res. 85 (2009) 199–205.
[4] B. Tu, N.G. Bazan., Hippocampal kindling epileptogenesis upregulates neuronal cyclooxygenase-2 expression in neocortex, Exp. Neurol. 179 (2003) 167–175.
[5] P.S. Buckmaster, F.E. Dudek, Network properties of the dentate gyrus in epileptic rats with hilar neuron loss and granule cell axon reorganization, J. Neurophysiol. 77 (1997) 2685–2696.

[6] G. Paxinos, C. Watson, The Rat Brain in Stereotaxic Coordinates, 6th ed, Academic Press/Elsevier, Amsterdam, Boston, 2007.

[7] K.K. Cole-Edwards, A.E. Musto, N.G. Bazan., c-Jun N-terminal kinase activation responses induced by hippocampal kindling are mediated by reactive astrocytes, J. Neurosci. 26 (2006) 8295–8304.

[8] R.J. Racine, Modification of seizure activity by electrical stimulation. II. Motor seizure, Electroencephalogr. Clin. Neurophysiol. 32 (1972) 281–294.

[9] W.T. Blume, G.B. Young, J.F. Lemieux., EEG morphology of partial epileptic seizures, Electroencephalogr. Clin. Neurophysiol. 57 (1984) 295–302.

[10] M.J. Lehmkuhle, K.E. Thomson, P. Scheerlinck, W. Pouliot, B. Greger, F.E. Dudek., A simple quantitative method for analyzing electrographic status epilepticus in rats, J. Neurophysiol. 101 (2009) 1660–1670.

[11] A.M. White, P.A. Williams, D.J. Ferraro, S. Clark, S.D. Kadam, F.E. Dudek, et al., Efficient unsupervised algorithms for the detection of seizures in continuous EEG recordings from rats after brain injury, J. Neurosci. Methods 152 (2006) 255–266.

[12] H.R. Mohseni, A. Maghsoudi, M.B. Shamsollahi, Seizure detection in EEG signals: a comparison of different approaches, Conf. Proc. IEEE Eng. Med. Biol. Soc. Suppl. (2006) 6724–6727.

[13] S.B. Wilson, R.N. Harner, F.H. Duffy, B.R. Tharp, M.R. Nuwer, M.R. Sperling, Spike detection. I. Correlation and reliability of human experts, Electroencephalogr. Clin. Neurophysiol. 98 (1996) 186–198.

[14] B.A. Gross, C.M. Walsh, A.A. Turakhia, V. Booth, G.A. Mashour, G.R. Poe, Open-source logic-based automated sleep scoring software using electrophysiological recordings in rats, J. Neurosci. Methods 184 (2009) 10–18.